

Article

# The Solar Reflectance Index as a Tool to Forecast the Heat Released to the Urban Environment: Potentiality and Assessment Issues

Alberto Muscio \* 

Energy Efficiency Laboratory, University of Modena & Reggio Emilia, Modena 41121, Italy; alberto.muscio@unimore.it; Tel.: +39-059-2056194

Received: 31 December 2017; Accepted: 13 February 2018; Published: 15 February 2018

**Abstract:** Overheating of buildings and urban areas is a more and more severe issue in view of global warming combined with increasing urbanization. The thermal behavior of urban surfaces in the hot seasons is the result of a complex balance of construction and environmental parameters such as insulation level, thermal mass, shielding, and solar reflective capability on one side, and ambient conditions on the other side. Regulations makers and the construction industry have favored the use of parameters that allow the forecasting of the interaction between different material properties without the need for complex analyses. Among these, the solar reflectance index (SRI) takes into account solar reflectance and thermal emittance to predict the thermal behavior of a surface subjected to solar radiation through a physically rigorous mathematical procedure that considers assigned air and sky temperatures, peak solar irradiance, and wind velocity. The correlation of SRI with the heat released to the urban environment is analyzed in this paper, as well as the sensitivity of its calculation procedure to variation of the input parameters, as possibly induced by the measurement methods used or by the material ageing.

**Keywords:** ageing; emissivity; measurement; solar reflectance; solar reflectance index; thermal emittance; urban heat island

---

## 1. Introduction

Overheating of buildings and urban areas is a more and more severe issue due to increasing urbanization combined with global warming. In fact, 54% of the world's population already lives in urban areas, and the percentage is expected to rise to 66% by 2050 [1]. In cities of any size the urban heat island (UHI) phenomenon shows up, which is the development of higher ambient temperatures compared to the surrounding rural and suburban areas: a recent study on one hundred Asian and Australian cities [2] reported average UHI intensities between 4.1 °C and 5.0 °C, and peaks of 11.0 °C. The UHI effect is also unfavorably superposed to the sharp increase of the mean global temperature observed in recent years [3]. In short, humanity is gathering in cities that are a lot warmer than the surrounding world, which is itself warming up!

A strong relationship exists between ambient temperature and mortality, with a threshold temperature above which mortality rates increase very rapidly and are considerably higher than the annual average [4]; such a threshold temperature is a function of local climate, architecture, and the physiological characteristics of the population. Moreover, for each degree of temperature increment, the increase of the peak electricity load was shown to vary between 0.45% and 4.6%, and the increase of total electricity consumption between 0.5% and 8.5% [5]. On the other hand, a proper design of urban surfaces based on the use of solar reflective materials for roofs and pavements has been known for decades to have great potential for the mitigation of building and urban overheating [6,7].

The thermal behavior of buildings in the hot seasons is the result of a complex balance of construction and environmental parameters such as insulation level, thermal mass, shielding, and solar reflective capability on one side, temperature, wind, and solar irradiance on the other side. Advanced software tools for dynamic simulation are generally needed to accurately predict thermal comfort and cooling energy needs, but their complexity of use makes it difficult to exploit them for preliminary selection of single building components. As a result, performance parameters of materials and building elements such as steady-state thermal transmittance, thermal mass, or solar reflectance, are often considered to operate a product comparison and, from that, a preliminary selection. Nonetheless, it is well known that making reference to distinct performance parameters independently of the installation context may be inadequate and sometimes misleading. For example, a low steady-state thermal transmittance may not prevent lightweight dark roofs from overheating and yielding a strong cooling load due to lack of inertia. Analogously, a relatively high solar reflectance may not prevent a roof surface from overheating if it is coupled with a low thermal emittance of the external surface, unless the solar reflectance is really high or a strong wind is blowing. Therefore, regulation makers and the construction industry have often favored the use of parameters such as the periodic thermal transmittance—which combines thermal insulation and thermal inertia [8]—and the solar reflectance index (SRI), in which all relevant surface properties are contemporarily taken into account [9]. Such composite parameters allow forecasting of the interaction between different material properties without the need of complex analyses.

This paper is focused on the SRI, which has raised significant interest thanks to its relative ease of calculation and, above all, its effective representation of the thermal behavior of opaque built surfaces subjected to solar radiation. In particular, it is contemplated by voluntary rating systems such as LEED [10], or regulations on energy efficiency such as Title 24 of California [11]. SRI is calculated from the solar reflectance and the thermal emittance of the analyzed surface through a physically rigorous procedure that considers assigned and highly demanding ambient conditions such as air and sky temperatures, wind velocity, and peak solar irradiance [9]. More specifically, this paper aims to analyze the correlation of SRI with the heat released to the near ground air, as well as the sensitivity of SRI calculation to variation in the input parameters, as possibly induced by the measurement methods or material weathering and soiling. The objective is to assess the potential of SRI as a tool to easily compare the performance of built surfaces in terms of heat released to the urban environment.

## 2. The Solar Reflectance Index (SRI) and Its Calculation

### 2.1. Surface Radiative Properties and SRI

The solar reflectance, or albedo, of a surface is the reflected fraction of incident solar radiation. It ranges from 0 to 1 (or 100%). Its value  $\rho_{\text{sol}}$  can be calculated by averaging over the range from 300 nm to 2500 nm, in which about 99% of total solar irradiance falls; the measured spectral reflectivity  $\rho_{\lambda}$ , defined as the ratio of reflected part and total amount of incident radiation at the considered wavelength  $\lambda$  (nm); weighted by the spectral irradiance of the sun at the earth surface,  $I_{\text{sol},\lambda}$  ( $\text{W}/(\text{m}^2 \text{ nm})$ );

$$\rho_{\text{sol}} = \frac{\int_{300}^{2500} \rho_{\lambda} \cdot I_{\text{sol},\lambda} \cdot d\lambda}{\int_{300}^{2500} I_{\text{sol},\lambda} \cdot d\lambda} \quad (1)$$

Minimum values of solar reflectance are specified in many countries by regulations on building energy efficiency such as Title 24 of California [11], as well as by voluntary programs incentivizing energy efficiency like the Energy Star of EPA [12]; those values are usually differentiated for low-sloped and steep-sloped roofs and, possibly, for building use (e.g., residential/nonresidential). Minimum values are often set also for another surface property, the thermal emittance (also called infrared emittance, or emissivity). This is the ratio of the energy emitted in the far infrared (i.e., in the range from 4 to 40  $\mu\text{m}$ ) toward the sky by the considered surface and the maximum theoretical emission

at the same surface temperature; this likewise ranges from 0 to 1 (or 100%). A low thermal emittance may cause a surface to overheat even if this is highly reflective because the fraction of solar radiation that is absorbed, however small it is, cannot be effectively released to the atmosphere. In many cases, however, only the solar reflectance or its complement to 1, the solar absorptance, are considered in regulations for opaque building elements.

The combined effect of different surface properties can be expressed through the “solar reflectance index” (SRI), a parameter calculated by the relationship [9]

$$SRI = 100 \cdot \frac{T_{sb} - T_{se}}{T_{sb} - T_{sw}}, \tag{2}$$

where  $T_{se}$  (K) is the temperature that the considered surface would steadily reach when irradiated by a reference solar flux  $I_{sol,max} = 1000 \text{ W/m}^2$  at atmospheric air temperature  $T_{air} = 310 \text{ K}$ ; sky temperature  $T_{sky} = 300 \text{ K}$ ; and convection heat transfer coefficient  $h_{ce}$  to which three different values are assigned, equal to 5, 12, and  $30 \text{ W/(m}^2 \text{ K)}$  for, respectively, low ( $v_{wind} < 2 \text{ m/s}$ ), intermediate ( $2 \text{ m/s} < v_{wind} < 6 \text{ m/s}$ ), and high ( $6 \text{ m/s} < v_{wind} < 10 \text{ m/s}$ ) wind speed. Intermediate wind speed is generally taken into account for product comparison.  $T_{sb}$  (K) and  $T_{sw}$  (K) are the temperatures that would be steadily reached by two reference surfaces, respectively, a black one ( $\rho_{sol,b} = 0.05$ ) and a white one ( $\rho_{sol,w} = 0.80$ ), with both surfaces having high thermal emittance ( $\epsilon_e = 0.90$ ) (see Figures 1 and 2).

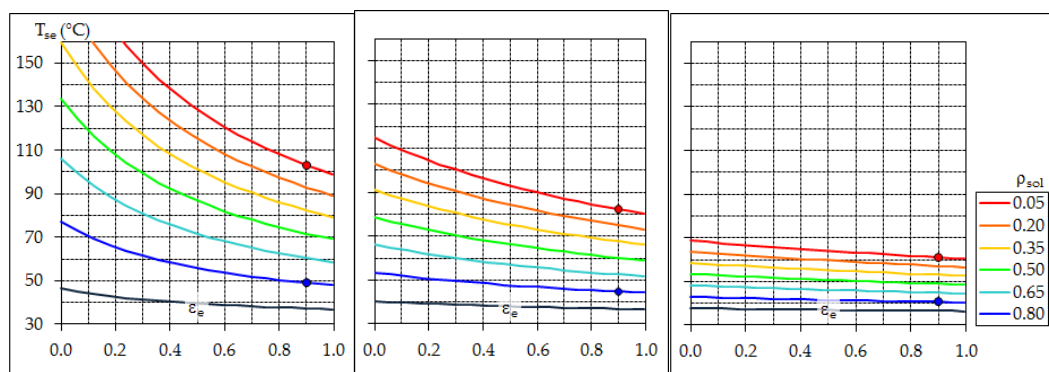


**Figure 1.** Surface temperature  $T_{se}$  for reference ambient conditions and (from left to right) low ( $v_{wind} < 2 \text{ m/s}$ ,  $h_{ce} = 5 \text{ W/(m}^2 \text{ K)}$ ), intermediate ( $2 \text{ m/s} < v_{wind} < 6 \text{ m/s}$ ,  $h_{ce} = 12 \text{ W/(m}^2 \text{ K)}$ ), and high ( $6 \text{ m/s} < v_{wind} < 10 \text{ m/s}$ ,  $h_{ce} = 30 \text{ W/(m}^2 \text{ K)}$ ) wind speed; blue and red dots are for the reference white and black surfaces, respectively.

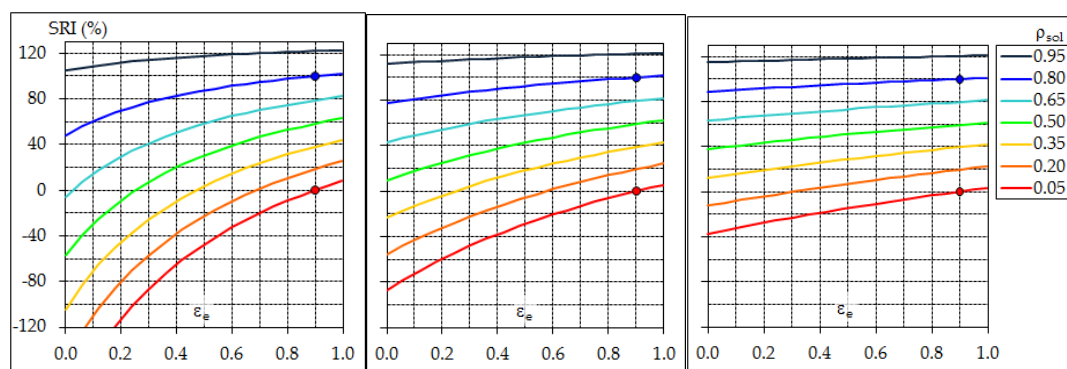


**Figure 2.** Solar reflectance index (SRI) for reference ambient conditions and (from left to right) low ( $v_{wind} < 2 \text{ m/s}$ ,  $h_{ce} = 5 \text{ W/(m}^2 \text{ K)}$ ), intermediate ( $2 \text{ m/s} < v_{wind} < 6 \text{ m/s}$ ,  $h_{ce} = 12 \text{ W/(m}^2 \text{ K)}$ ), and high ( $6 \text{ m/s} < v_{wind} < 10 \text{ m/s}$ ,  $h_{ce} = 30 \text{ W/(m}^2 \text{ K)}$ ) wind speed; blue and red dots are for the reference white and black surfaces, respectively.

SRI represents the temperature decrement that the analyzed surface would allow with respect to the reference black surface in the reference ambient conditions, divided by the analogous decrement allowed by the reference white surface, eventually given in percentage terms. The surface temperature  $T_{se}$  (as well as  $T_{sb}$  and  $T_{sw}$ ) is determined by iteratively solving the following heat balance, based on the hypothesis of an adiabatic irradiated surface:

$$(1 - \rho_{sol}) \cdot I_{sol} = \varepsilon_e \cdot \sigma_0 \cdot (T_{se}^4 - T_{sky}^4) + h_{ce} \cdot (T_{se} - T_{air}) \quad (3)$$

SRI takes into account either the solar reflectance  $\rho_{sol}$  or the thermal emittance  $\varepsilon_e$ , as well as the reference wind velocity through the convection coefficient  $h_{ce}$ . Even if expressed in percent, its definition allows for values lower than zero or higher than 100 since materials worse than the black reference surface, or better than the white reference surface, can exist. The plots in Figures 1 and 2 show that high values of both solar reflectance and thermal emittance are contemporarily needed to obtain a low overheating of the involved surface in all wind conditions, unless its solar reflectance is really high.

## 2.2. Potentiality and Limitations of SRI

SRI matches the need of a single performance parameter as it allows to easy comparison of the performance of different solar reflective solutions. When applied to roofs and pavements, it is a clear indicator of the capability of their surface to return the incident solar radiation to the atmosphere by direct reflection and far infrared radiation. SRI does not take into account the sky view factor of urban surfaces nor the canyon effect, so it is mostly significant with regard to pavements and horizontal or low-slope roofs with a sky view factor close to 1. In such cases, the reflected part of solar radiation and the far-infrared thermal radiation emitted by roof and pavement surfaces can reach the high atmosphere and, therefore, the contribution to ambient warming at ground level is mostly due to convection heat transfer to the near ground air, whose rate per unit surface can be evaluated as follows:

$$q_{ce}'' = h_{ce} \cdot (T_{se} - T_{air}) \quad (4)$$

Given the temperatures of the black and white reference surfaces,  $T_{sb}$  and  $T_{sw}$ , in the ambient conditions assigned for SRI calculation, the fraction of incident solar radiation that is transferred to the near ground air can be evaluated from the definition in Equation (2) combined with Equation (4) as follows:

$$\frac{q_{ce}''}{I_{sol}} = \frac{1}{I_{sol}} \cdot h_{ce} \cdot \left[ T_{sb} - \frac{SRI}{100} \cdot (T_{sb} - T_{sw}) - T_{air} \right] \quad (5)$$

Figure 3 shows that, being assigned the local wind velocity, a linear correlation exists between SRI and both the surface temperature  $T_{se}$  and the fraction of incident solar heat that is transferred to the near ground air. Since a given SRI value can be the result of different pairs of solar reflectance and thermal emittance values, as shown in Figure 2, SRI seems a more effective indicator of the capability of a surface to limit urban warming than solar reflectance alone. In fact, while thermal emittance of urban surfaces is generally around 0.9, metal roof panels with bare metal finish or thin coating and, consequently, much lower thermal emittance are often used in tropical and warm areas.

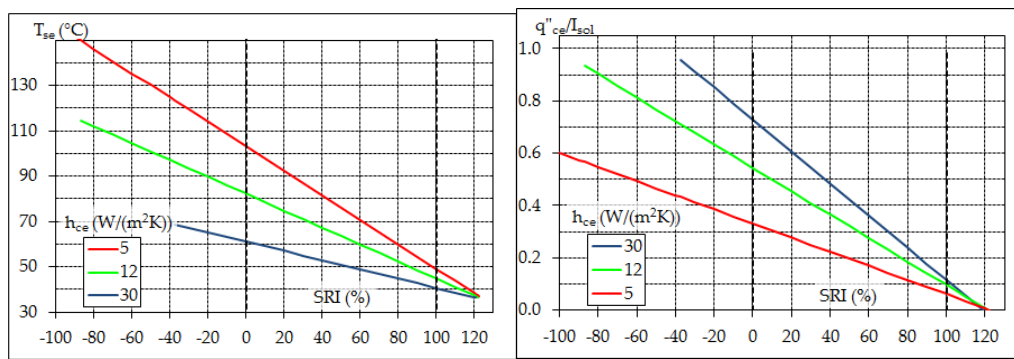


**Figure 3.** Surface temperature  $T_{se}$  (left) and fraction of incident solar heat transferred to the near ground air (right) vs SRI with convection coefficient  $h_{ce}$  for low, intermediate, or high wind speed and other standard conditions for SRI calculation ( $I_{sol} = 1000 \text{ W/m}^2$ ,  $T_{air} = 310 \text{ K}$ ,  $T_{sky} = 300 \text{ K}$ ).

SRI is based on the hypothesis of an adiabatic irradiated surface and does not consider the insulation or the inertia of the materials below, nonetheless it can again work well as an indicator of the heat transmitted by convection to the external near ground air because the heat flow rate conducted to the ground or through a roof can be lower by one or two orders of magnitude than solar irradiance. Regarding the heat flow rate entering an inhabited space below a roof, this one and the ceiling surface temperature, relevant to indoor thermal comfort, can again be correlated to  $T_{se}$ . In particular, the heat transmitted into the inhabited space is the result of the dynamic behavior of the roof structure with its insulation and thermal mass while subjected to the solar cycle, so in principle it must be calculated through mathematical tools such as the quadrupole method specified in EN ISO 13786 [8], or numerical simulation. This issue has been addressed with the recently proposed Solar Transmittance Index (STI) [13], which extrapolates the SRI approach by comparing the peak of oncoming heat flow rate (as resulting from the surface and bulk properties of the roof) with that obtained for two low- and high-performance reference cases; STI is currently under development in the specific aspect of identifying the reference cases. Nevertheless, for many roofing solutions with very low thermal inertia such as the commonly used corrugated metal panels or insulated sandwich panels, quasi-steady state conditions can be assumed throughout the day and, in particular, when the peak of solar irradiance occurs. In particular, given the indoor temperature  $T_i$  (°C), the R factor ( $\text{m}^2 \text{ K/W}$ ) of the roof, and the inner surface resistance  $R_{si}$  ( $\text{m}^2 \text{ K/W}$ ) as resulting from convection and far-infrared radiation heat transfer, the transmitted heat flux  $q_i$  ( $\text{W/m}^2$ ) can be estimated as follows:

$$q_i = \frac{T_{se} - T_i}{R + R_{si}} \tag{6}$$

Consequently, a heat balance can be extrapolated for the roof from that developed for adiabatic surfaces as presented in Equation (3):

$$(1 - \rho_{sol}) \cdot I_{sol} = \epsilon_e \cdot \sigma_0 \cdot (T_{se}^4 - T_{sky}^4) + h_{ce} \cdot (T_{se} - T_{air}) + \frac{T_{se} - T_i}{R + R_{si}} \tag{7}$$

Iteratively solving the heat balance in Equation (7) with respect to  $T_{se}$  for common values of the R factor yields a very low change of SRI from that of an adiabatic surface (i.e.,  $\Delta SRI = SRI_{nonadiabatic} - SRI_{adiabatic}$ ), especially for common surfaces with high thermal emittance ( $\Delta SRI < 0.01$  for  $\epsilon_e > 0.75$ ) (Figure 4). A confirmation is thus obtained that the SRI can be an excellent parameter for product comparison even for non-adiabatic surfaces. Moreover, a verification is provided to the hypothesis that the peak of transmitted heat flow rate is much lower than the absorbed solar irradiance and, consequently, much lower than the total irradiance (Figure 5).

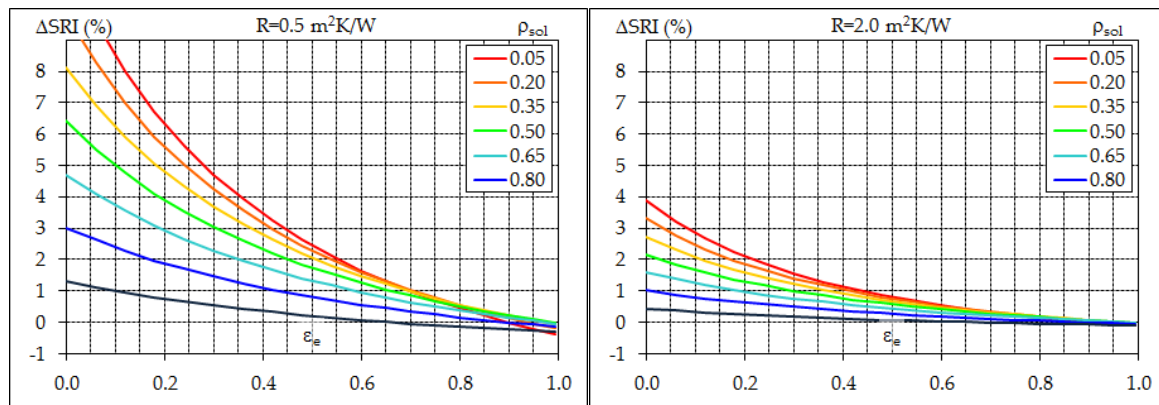


**Figure 4.** Change of SRI for a non-adiabatic roof surface with respect to an adiabatic one for  $T_i = 27\text{ }^\circ\text{C} \cong 300\text{ K}$ ,  $R_{si} = 0.17\text{ m}^2\text{ K/W}$ ,  $h_{ce} = 12\text{ W}/(\text{m}^2\text{ K})$  and (from left to right) uninsulated ( $R \approx 0.5\text{ m}^2\text{ K/W}$ ) and well insulated ( $R \approx 2.0\text{ m}^2\text{ K/W}$ ) roofs, both with negligible thermal mass.

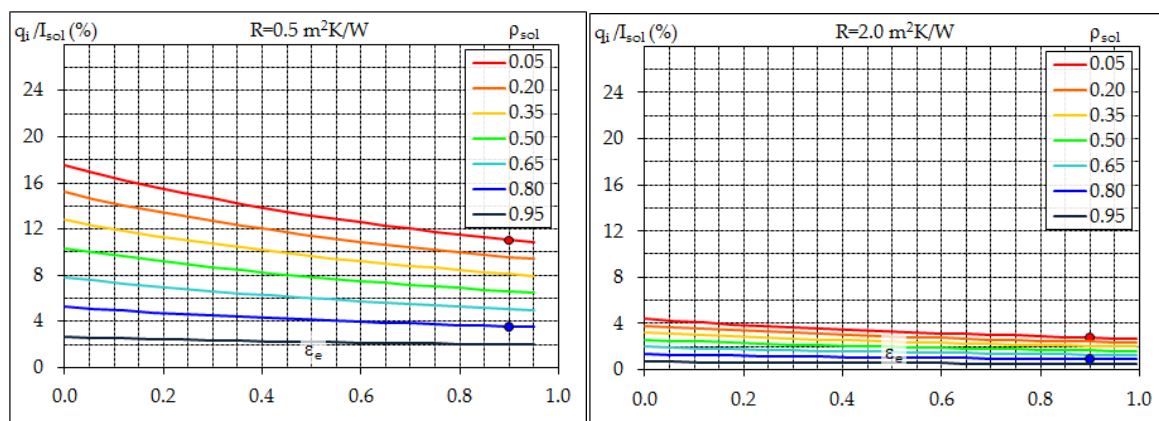


**Figure 5.** Ratio of peak transmitted heat flow rate and solar irradiance for  $T_i = 27\text{ }^\circ\text{C} \cong 300\text{ K}$ ,  $R_{si} = 0.17\text{ m}^2\text{ K/W}$ ,  $h_{ce} = 12\text{ W}/(\text{m}^2\text{ K})$  and (from left to right) uninsulated ( $R \approx 0.5\text{ m}^2\text{ K/W}$ ) and well insulated ( $R \approx 2.0\text{ m}^2\text{ K/W}$ ) roofs, both with negligible thermal mass.

In brief, SRI has found a strong interest in the construction sector in view of its effectiveness of representation of the surface behavior. As already stated, it is contemplated by voluntary rating systems such as LEED when dealing with the summer performance of opaque roof elements and pavements: initial values of  $\text{SRI} \geq 82$  for low-sloped roofs (slope  $\leq 2:12$  or  $9.5^\circ$ ),  $\text{SRI} \geq 39$  for steep-sloped roofs, or  $\text{SRI} \geq 33$  for pavements and other non-roof surfaces are required in the U.S. [10]. 2016 Title 24 of California [11] permits the SRI instead of separately considering solar reflectance and thermal emittance when complying with requirements on building energy efficiency.

The SRI calculation procedure is currently specified by an ASTM Standard, but a derivative European Standard is also under development. Radiative properties from which SRI is calculated, and the SRI itself, can be rated through bodies like the Cool Roof Rating Council of the U.S. [14] or the European Cool Roof Council [15]. Figure 6 shows the number of samples tested since 2014 by the Energy Efficiency Laboratory (EELab) at Modena, an accredited ECRC test laboratory; since 2015 the tests have been performed mostly under ISO/IEC 17025 accreditation [16] and some of them for ECRC rating. The sharp increase in the total number of tested samples testifies to the increasing interest for solar reflective solutions in Europe, which may rapidly approach that in the U.S. Moreover, the high fraction of tests aimed at SRI assessment testifies for the interest of the construction sector in this specific parameter.

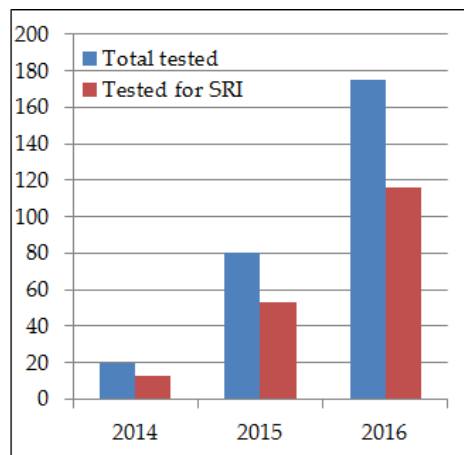


**Figure 6.** Samples tested at EELab for assessment of surface properties.

An issue regarding the determination of SRI may concern the arbitrary identification of the convection heat transfer coefficient at the external surface. Different measurement methods can also be used to determine solar reflectance and thermal emittance, providing slightly different results and thus affecting the SRI value. Moreover, aged values of the surface properties, the solar reflectance above all, may be significantly lower than initial values due to weathering and soiling. All these issues and their potential impact on SRI are analyzed in the following section.

### 3. Sensitivity of SRI Calculation to Input Parameters, and Measurement Issues

#### 3.1. External Convection Coefficient

ASTM E1980 [9] proposes a kind of step function to estimate the convection coefficient  $h_{ce}$  to be used for SRI calculation (Figure 7). Since  $h_{ce}$  has a significant impact on the value of  $T_{se}$  and, from that, on SRI, a comparison has been made here between ASTM E1980 specifications and the literature. In this regard, EN ISO 6946 [17], a standard calculation method commonly used in the construction sector of Europe, correlates  $h_{ce}$  to the wind velocity  $v_{wind}$  (m/s) through the following empirical relationship:

$$h_{ce} = 4 + 4 \cdot v_{wind} \quad (8)$$

The formula yields higher values than those in ASTM E1980 (Figure 7), but EN ISO 6946 is presumably focused onto winter conditions, relevant to building heating, so it is supposed to adopt a precautionary approach that overestimates heat loss. More specialized literature on single phase convection heat transfer, summarized in [18] and other reference handbooks [19,20], proposes the following relationship for natural convection as induced by buoyancy forces on a horizontal plate with hot top:

$$Nu_n = 0.15 \cdot Ra^{1/3} \quad (9)$$

The Nusselt number  $Nu_n$  is the dimensionless form of the natural convection heat transfer coefficient  $h_{ce,n}$

$$Nu_n = \frac{h_{ce,n} \cdot L_n}{\kappa} \quad (10)$$

and  $Ra$  is the Rayleigh number, defined as follows:

$$Ra = \frac{g \cdot b \cdot \Delta T \cdot L_n^3}{\nu \cdot \alpha} \quad (11)$$

The formula in Equation (9) is valid for  $10^7 < Ra < 10^{11}$ . Thermal conductivity  $\kappa$  (W/(m·K)), cinematic viscosity  $\nu$  (m<sup>2</sup>/s) and thermal diffusivity  $\alpha$  (m<sup>2</sup>/s) of the air are evaluated at the film

temperature—that is, the average of surface and air temperature—whereas the coefficient of thermal expansion  $b$  ( $K^{-1}$ ) is the inverse of the absolute temperature of the air  $T_{air}$ , in kelvin. The temperature difference  $\Delta T = T_{se} - T_{air}$  ( $^{\circ}C$ ) is that between the plate surface and the air, the reference length  $L_n$  (m) is the ratio of plate area and perimeter, and  $g$  is gravity.

The following relationship is also proposed in the literature [18–20] for forced convection heat transfer on a horizontal flat plate with a turbulent boundary layer that begins at the leading edge:

$$Nu_f = 0.037 \cdot Re^{4/5} \cdot Pr^{1/3} \quad (12)$$

The Nusselt number  $Nu_f$  is the dimensionless form of the forced convection heat transfer coefficient  $h_{ce,f}$  averaged over the plate

$$Nu_f = \frac{h_{ce,f} \cdot L_f}{\kappa} \quad (13)$$

and the Reynolds number  $Re$  includes the undisturbed wind velocity:

$$Re = \frac{v_{wind} \cdot L_f}{\nu} \quad (14)$$

The formula in Equation (12) is valid for  $5 \cdot 10^5 < Re < 10^7$ . The Prandtl number  $Pr$  and the other thermal properties of the air are again evaluated at the film temperature. The reference length  $L_f$  (m) is the length of the plate in the direction of fluid flow.

When natural convection and forced convection are superposed and have the same order of magnitude, a mixed convection Nusselt number can be evaluated as follows:

$$Nu^n = Nu_f^n \pm Nu_n^n \quad (15)$$

If buoyancy-induced flow and forced flow have the same or transverse direction, a case of assisting or transverse flow occurs, respectively, and the + applies, otherwise the – applies for opposing flow. For the exponent  $n$  the most used value is 3, however for the case of transverse flow over flat plates  $n = 3.5$  may provide a better correlation of data [19,20]. In principle, the reference length should be the same ( $L_n = L_f = L$ ), but for Equation (9) and Equation (12) it is not. In order to overcome such issues, the following relationship can be extrapolated from Equation (15) to combine the natural and forced convection coefficients (for transverse flow):

$$h_{ce}^n \approx h_{ce,f}^n + h_{ce,n}^n \quad (16)$$

In Figure 7 the convection coefficient calculated according to the different estimate methods is plotted against the wind velocity at ambient reference conditions for SRI calculation and sea level air properties. For calculation of  $h_{ce}$  by means of Equation (16) a horizontal roof surface  $10 \text{ m} \times 10 \text{ m}$  or  $20 \text{ m} \times 20 \text{ m}$  is considered, as well  $n = 3.5$  and two different values of the temperature difference  $\Delta T = T_{se} - T_{air}$ , equal to  $5 \text{ }^{\circ}C$  and  $20 \text{ }^{\circ}C$ . For intermediate and high wind conditions, forced convection seems to dominate natural convection and the influence of  $\Delta T$  on  $h_{ce}$  is very low or negligible. The reference values of  $h_{ce}$  specified by ASTM E1980 are halfway between those calculated according to EN ISO 6946 and the empirical formulas from the literature. Indeed the choice of  $h_{ce}$  is arbitrary since its actual value is a complex function of building shape, wind velocity and direction, and local ambient conditions; thus, one can conclude that ASTM E1980 provides arbitrary, but reasonable, values. Moreover, for those values, SRI permits an effective comparison of roofing and pavement solutions based on their radiative properties since variations of such properties have a negligible effect on  $h_{ce}$  for products which have similar performance.

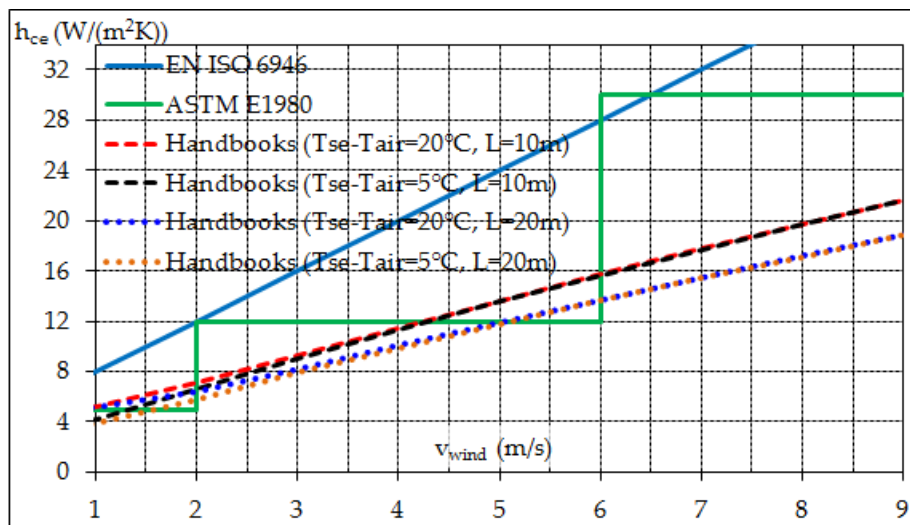


Figure 7. Convection coefficient vs. wind velocity according to different estimation methods.

### 3.2. Assessment of Solar Reflectance and Ageing Issues

Solar reflectance can be measured through Equation (1) by means of several methods, based on spectrophotometers [21–24] or solar reflectometers [23–25]. Independently of the method and instrument used, a main issue is the choice of the reference solar spectrum with which the average of the reflectivity spectrum is weighted. The correlation pattern of solar irradiance versus wavelength depends on parameters such as air mass (ratio of the mass of atmosphere in the actual observer-sun path to the mass that would exist if the observer were at sea level, at standard barometric pressure, and the sun were directly overhead), orientation and inclination of the irradiated surface, inclusion of direct, circumsolar or global (i.e., direct and diffuse) irradiance, position of the sun in the sky, sky conditions, etc. Among the many standard spectra available (Figure 8), the one initially recommended by the ASTM E903 Standard [21] in its 1996 version and thus considered by the Cool Roof Rating Council of U.S. [14] for product rating, also permitted by the European Cool Roofs Council [15], is that specified by the ASTM E891 Standard [26] for air mass 1.5 and beam normal solar irradiance (i.e., solar flux coming from the solid angle of the sun's disk on a surface perpendicular to the axis of that solid angle), designated 'E891BN' in the following. Such a spectrum was presumably intended for sun-tracking photovoltaic panels at the latitude of the U.S. and it may not be the most proper choice when the thermal behavior of a built surface subjected to solar radiation is considered. Moreover, ASTM E891 has been withdrawn and substituted by ASTM G173 [27], nevertheless E891BN is still largely use for product rating, most likely for ease and fairness of comparison with already rated products. The current version of ASTM E903 recommends the couple of spectra reported in ASTM G173, again for air mass 1.5 and for direct circumsolar irradiance (i.e., solar flux coming from a solid angle with aperture half-angle of  $2.9^\circ$  centered on the sun's disk) or global irradiance (i.e., direct and diffuse solar flux coming from the whole hemisphere overhead) on a sun-facing  $37^\circ$  tilted surface, in the following designated 'G173DN' and 'G173GT', respectively. Also these spectra are probably intended for use with sun tracking or fixed photovoltaic panels at the latitude of the U.S. In recent research on solar reflective built surfaces [23,24], the air mass 1 global horizontal spectrum, considering direct and diffuse radiation on a horizontal surface with the sun directly overhead in clear sky, here designated 'AM1GH', has been recommended as the spectrum of choice. Using AM1GH allows the measurement of solar reflectance under conditions that best predict annual peak solar heat gain, which is helpful because air conditioning systems are typically sized to meet annual peak cooling load. Moreover, electric grid peak load and health issues mostly arise for annual peak cooling load. While optimal for horizontal surfaces at mainland U.S. latitudes, AM1GH was shown to also apply well to moderately pitched roofs with a slope up to  $23^\circ$ , moreover it is expected to work well from  $49^\circ$  S to  $49^\circ$  N [23]. In the European Union a similar

spectrum of global irradiance for air mass 1 is specified in the EN 410 Standard [22], intended for testing of window glass and designated 'EN410G' in the following. The use of such types of spectrum seems to be confirmed in the draft of a standard test method for solar reflectance measurement that is currently under development. In Table 1 the percent energy content of the different spectra in the UV (ultraviolet), visible (Vis) and near infrared (NIR) ranges is also summarized. Of course further spectra may be considered [23].

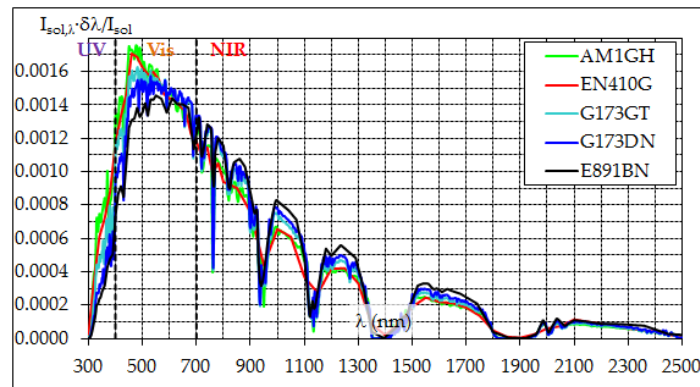


Figure 8. Standard solar irradiance spectra, normalized.

Table 1. Energy content (%) of solar spectra in the UV-Vis-NIR ranges.

	AM1GH	EN410G	G173GT	G173DN	E891BN
UV (300–400 nm)	6.8	6.4	4.7	3.5	3.0
Vis (400–700 nm)	44.7	44.1	43.3	42.0	39.0
NIR (700–2500 nm)	48.5	49.5	52.0	54.5	58.0

The solar spectra presented here, shown in Figure 5, clearly have different spectral contents. One can integrate them from 300 nm to a given wavelength  $\lambda$  in order to calculate the fraction of total irradiance included in the spectral range from 300 nm to  $\lambda$ ,  $F_{300 \rightarrow \lambda}$ , thus obtaining the plots in Figure 9. These show that, at the boundary between visible and NIR (commonly set at 700 nm for analyses on solar reflective materials) there is up to 10% of difference, in terms of cumulated energy content, between air mass 1 global horizontal spectra such as AM1GH and EN410G, and direct/beam normal spectra such as E891BN or G173DN. One can also see in Table 1 that the NIR content of E891BN (evaluated as  $1 - F_{300 \rightarrow 700}$ ) is as high as 58%, whereas it is slightly lower than 50% for air mass 1 spectra such as AM1GH and EN410G. This means that a selective material highly absorbent in the visible range, for example due to a dark color mandatory for the considered built surface, but at the same time highly reflective in the NIR range, may be rated differently as a result of the selected reference spectrum.

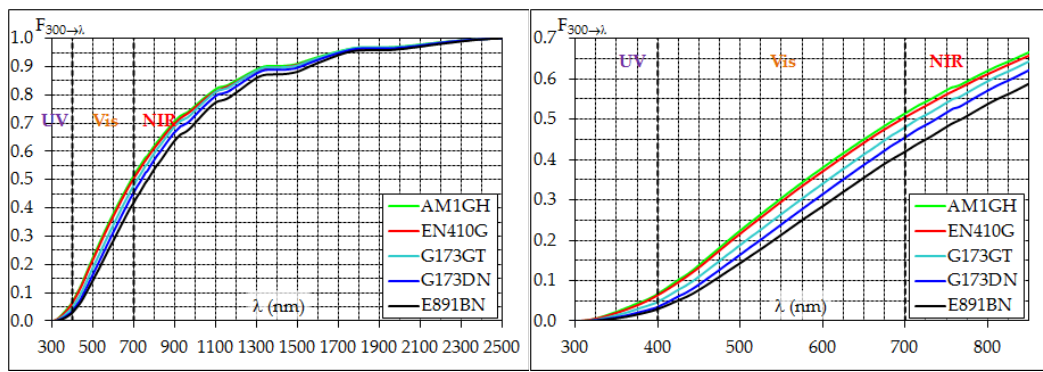


Figure 9. Cumulative energy content vs wavelength (full spectra and close-up on UV-VIS).

An experimental campaign was carried out at EELab on a set of samples representative of different product types and colors, summarized in Figure 10 and Table 2. In agreement with other research [23], selective surfaces such as samples 0218 and 0219, having NIR reflectance clearly higher than visible reflectance (Figure 11), yielded a difference as large as 0.04 between the lowest reflectance values returned by using EN410G (similar to AMIGH) and the highest ones returned by using E891BN. The same occurs, at a lesser extent, for samples 0220 and 0004, which show a highly variable reflectivity spectrum over the range relevant to solar radiation. The lowest difference occurs for a flat spectrum such as that of sample 0011. A lower difference exists, but still in favor of E891BN, between this and G173GT, whereas the situation with G173DN is about halfway. It is also worth noting that measurements made according to ASTM C1549 [25], which are carried out by an instrument with broadband sensors that fundamentally implement Equation (1) and allows selection of a weighting solar spectrum among the most commonly used ones, returns similar but slightly lower and thus precautionary values than truly spectrophotometric measurements (Table 2). In the authors’ knowledge, only one instrument compliant with ASTM C1549 is commercially available.



Figure 10. Sample set tested at EELab.

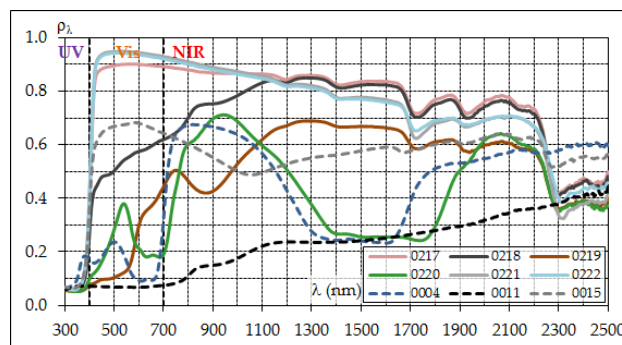


Figure 11. Measured reflectivity spectra.

**Table 2.** Measured solar reflectance values.

Lab. Code	Sample Description	Reference Solar Spectrum			
		EN410G	G173GT	G173DN	E891BN
0217	Elastomeric water based paint on aluminum	0.816	0.826	0.836	0.839
		-	0.799	0.810	0.815
0218	Elastomeric water based paint on aluminum	0.612	0.625	0.637	0.650
		-	0.606	0.623	0.635
0219	Elastomeric water based paint on aluminum	0.359	0.372	0.385	0.401
		-	0.367	0.380	0.389
0220	Elastomeric water based paint on aluminum	0.357	0.367	0.377	0.388
		-	0.358	0.367	0.378
0221	Elastomeric water based paint on aluminum	0.835	0.845	0.853	0.854
		-	0.817	0.826	0.828
0222	Elastomeric water based paint on aluminum	0.828	0.838	0.846	0.848
		-	0.815	0.824	0.830
0004	Engobed ceramic til	0.347	0.356	0.365	0.377
		-	0.348	0.354	0.364
0011	Engobed ceramic til	0.125	0.128	0.132	0.138
		-	0.125	0.128	0.133
0015	Engobed ceramic til	0.577	0.583	0.588	0.589
		-	0.564	0.570	0.570

Note: data in italic were measured by a solar reflectometer compliant with ASTM C1549 [25].

When dealing with rating of commercial products, a few percentage points of difference generated by the selection of the reference spectrum rather than the true product performance may unfairly influence the choice of designers and end users. This is presumably the reason why the E891BN spectrum is still in use though ASTM E891 [26] was withdrawn in 1999. On the other hand, it seems reasonable to measure solar reflectance under conditions that best predict the annual peak of solar heat gain, that is when the sun is high in a cloudless sky and irradiates horizontal or low-pitched surfaces, so spectra such as AM1GH or EN410G should be preferred. Their adoption, however, would artificially lower the measured performance of newly rated products, so a correction would be needed to allow a fair comparison with previously rated ones. This could be accomplished in terms of a clear separation of values rated with the two different types of spectrum in two different sections of the databases of the qualification bodies, to be contemporarily implemented by all relevant bodies in the world to take care of globalization, also showing in the databases and/or the test reports/commercial specifications of newly rated products a clear statement on the maximum expected penalization with respect to the previous rating approach, of course to be quantified. Best wishes to people in charge of that!

An issue even more relevant than that regarding the reference solar spectrum is probably the effect of ageing of solar reflective products due to weathering and soiling. Significant studies [28,29] have shown that many products suffer significant loss of solar reflectance after a few years of ageing, especially those with high initial values of the reflectance. In the U.S. aged samples can be obtained by exposition in three different weathering sites accredited by CRRC [14], representative of three different climates. Aged solar reflectance, thermal emittance and SRI values can eventually be calculated as the mean of those obtained for samples weathered in the three sites. Indeed, the LEED rating system requires in the U.S. [10] not only initial values as previously mentioned, but also three-years aged values such that  $SRI \geq 64$  for low-sloped roofs,  $SRI \geq 32$  for steep-sloped roofs,  $SRI \geq 28$  for pavements and other non-roof surfaces. 2016 Title 24 of California [11] does not consider initial properties at all, but it requires minimum values of aged properties; more specifically, three-years aged values of  $SRI \geq 64$  or 75 (depending on the building use) are required for low-sloped roofs and  $SRI \geq 16$  for steep-sloped roofs.

In case three-years aged values of surface properties are not available, the following provisional formula has been proposed to predict the aged solar reflectance  $\rho_{sol,aged}$  from the initial value  $\rho_{sol,init}$  [29] by the formula

$$\rho_{sol,aged} = \rho_{sol,0} + \beta \cdot (\rho_{sol,init} - \rho_{sol,0}) \tag{17}$$

where  $\rho_{sol,0}$  is the solar reflectance of an opaque soil layer, and  $\beta$  is the resistance to soiling of the considered surface. With  $\beta = 1$  the surface does not change its reflectance after ageing, whereas with  $\beta = 0$  the aged reflectance becomes equal to that of the soil. The higher the initial reflectance, the larger is its expected decay. Values of  $\rho_{sol,0} = 0.20$  and  $\beta = 0.70$  were initially proposed in the 2008 Title 24 of California, but subsequent analyses on a large set of aged products rated in the CRRC and EPA databases [29] showed that actual values generally over-predict the aged reflectance returned by Equation (17) and thus suggested using product specific values of  $\beta$ , ranging from 0.76 for field-applied coatings to close to unity for factory-applied coatings. 2016 Title 24 [11] specifies  $\beta = 0.65$  for a field-applied coating and  $\beta = 0.70$  for not a field-applied coating in order to have a precautionary (but arbitrary) over-prediction. The effects of the latter values on SRI decay are summarized in Figure 12, where initial and aged SRI values are also shown for a surface such as the white reference one for SRI calculation, for which  $SRI = 100$ ; a change  $\pm 0.05$  is also considered for thermal emittance, more extensively explained in Section 3.3.

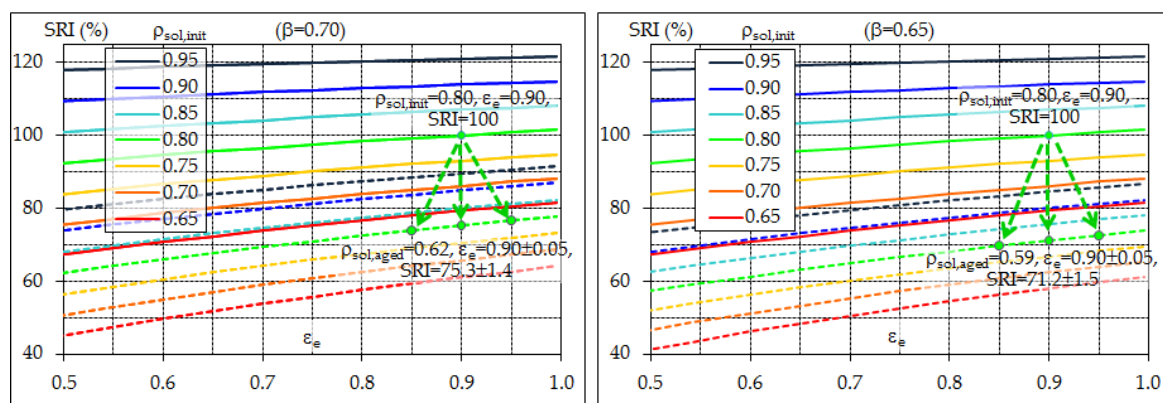


**Figure 12.** Initial (continuous lines) and aged (dashed lines) SRI values of highly reflective surfaces ( $\rho_{sol,init} \geq 0.65$ ) for intermediate wind speed ( $2 \text{ m/s} < v_{wind} < 6 \text{ m/s}$ ,  $h_{ce} = 12 \text{ W}/(\text{m}^2 \text{ K})$ ) and (from left to right) resistance to soiling  $\beta = 0.70$  and  $\beta = 0.65$ , with soil solar reflectance  $\rho_{sol,0} = 0.20$ .

Indeed, the significant scattering of data obtained for products naturally aged in the weathering sites of CRRC [29] suggests that measurements on aged samples are necessary to obtain the aged solar reflectance of each specific product. Nonetheless at least three years of natural ageing are needed, a requisite that is not easily accepted by the industry. Moreover, randomly variable conditions are always possible in the weathering sites due to variations in meteorology and air pollution, and this may affect significantly the results. The solution seems to be provided by a recently developed laboratory method for accelerated ageing [30,31]—already a standard test method as ASTM D7897 [32]—which can condense into three days the three-year long process of natural ageing used by the CRRC to rate roofing products sold in the U.S. Entering into details, a calibrated aqueous soiling mixture of dust minerals, black carbon, humic acid, and salts is sprayed onto  $10 \text{ cm} \times 10 \text{ cm}$  preconditioned coupons of the tested materials, which are then subjected to cycles of ultraviolet radiation, heat, and water in a commercial weatherometer. The method proved to be easy and fast to perform, repeatable, and above all able to reproduce the reflectance obtained in a wide range of naturally exposed roofing products [30,31].

In many countries different from the U.S. the regulations on solar reflective materials are still under development and only initial values of surface properties are generally considered. Moreover, only producers selling in the U.S. already have three-years aged samples, which are commonly unavailable

elsewhere for locally built and/or country specific products. On the other hand, a fast improvement of regulations and commercial products may be impeded by the long time required for natural ageing, moreover heavily polluted areas of Europe are probably not perfectly represented by the weathering sites of the U.S. The accelerated soiling method of ASTM D7897, possibly verified against local climate and pollution levels by means of validation studies, can thus provide a powerful tool to support the improvement of both regulations and product quality.

A short note can be made on ASTM E1918 Standard [24,33], a measurement method that compares the direct and reflected irradiances measured by a couple of pyranometers facing upwards and downwards, respectively, in order to retrieve the solar reflectance value. It is an effective method, especially for field measurements and if these are needed to calibrate mathematical models where the reflectance relevant to the current solar spectrum is concerned. Nonetheless it uses the randomly variable spectrum of the place and time of measurement, therefore it may not be the ideal choice for product rating and certification of the SRI.

### 3.3. Assessment of Thermal Emittance

It has already been evidenced that high values of thermal emittance allow rejection of solar energy absorbed by irradiated opaque surfaces [34], especially in low wind conditions. Solar reflectance is the key parameter to limit overheating, but a low thermal emittance may also affect re-emission of the absorbed solar energy and, therefore, the SRI. This is the case of uncoated metal surfaces, which can warm up as much as black roofing materials [35–38]. In this regard, regulations such as 2016 Title 24 of California [11] require minimum values of both solar reflectance and thermal emittance—higher than 0.75 for the latter—unless compliance is verified for their combination through the SRI.

Several test methods are available to measure thermal emittance, but most of them can be used only in the laboratory, often on small specimens made of pure materials, therefore they are of low practical usefulness in the construction industry. Only two methods seem available for measurement on actual building elements, usable with relative ease either in the laboratory or in the field. These are specified in the ASTM C1371 Standard [39] and the EN 15976 Standard [40]. To the authors' knowledge, only one instrument compliant with each test method is commercially available.

The emissometer based on ASTM C1371, called 'thermal emissometer' in the following, is probably the most used one, endorsed for performance assessment of solar reflective materials by both CRRC of the U.S. and ECRC (which, however, allows using also the alternative emissometer based on EN 15976). The total hemispherical emittance of the sample surface is evaluated through the following relationship [39]:

$$\Delta V = k \cdot \frac{\sigma_0 \cdot (T_d^4 - T_s^4)}{1/\epsilon_s + 1/\epsilon_d - 1} \quad (18)$$

In the above formula, the voltage signal  $\Delta V$  (V) is that returned by a differential thermopile sensor embedded in the instrument head, which is placed onto the sample and left there until a steady output is reached.  $\Delta V$  is proportional by a calibration constant  $k$  to the radiative heat flux exchanged between the bottom surface of the head and the sample surface. The former has assigned thermal emittance  $\epsilon_d$  and absolute thermodynamic temperature stabilized at an assigned value  $T_d$  (K), significantly higher than that of the analyzed surface ( $T_d > T_s$ ) and the ambient. The latter surface has thermal emittance  $\epsilon_s$  unknown and absolute thermodynamic temperature stabilized at a value  $T_s$  (K) as close as possible to the ambient. The calibration constant  $k$  multiplies the heat flux exchanged by thermal radiation between the two surfaces, which are assumed to be flat, parallel, virtually infinite and facing each other, as well as gray and diffusive. The emissometer is calibrated before each test by measuring two reference samples with known thermal emittance, respectively equal to  $\epsilon_{low}$  (for which a voltage signal  $\Delta V_{low}$  is yielded) and  $\epsilon_{high}$  (for which  $\Delta V_{high}$  is yielded). Linearity of the instrument

and uncertainty  $\pm 0.01$  are ensured in the range  $0.03 < \varepsilon_s < 0.93$  by the producer of the emissometer (which provided two reference samples with declared emittances  $\varepsilon_{\text{low}} = 0.06$  and  $\varepsilon_{\text{high}} = 0.87$ ), so that:

$$\varepsilon = \varepsilon_{\text{low}} + \left( \varepsilon_{\text{high}} - \varepsilon_{\text{low}} \right) \cdot \frac{\Delta V - \Delta V_{\text{low}}}{\Delta V_{\text{high}} - \Delta V_{\text{low}}} \quad (19)$$

The instrument indeed measures something between normal and hemispherical emittance, nonetheless it was shown to yield the hemispherical emittance value when the hemispherical emittances of the reference samples are interpolated [41,42]. If the tested sample has a non-negligible resistance to heat transfer, due to a low thermal conductivity of the support material, the heat input applied by the hot emissometer head to the sample surface induces a thermal gradient across the thickness of the sample itself. As a result, the temperature  $T_s$  of the sample surface rises to a value significantly higher than that of the ambient. In such cases, the actual value of thermal emittance can be recovered by using one among the modifications of the standard method suggested by the producer of the emissometer, among which the most commonly used one is the so-called ‘slide method’ [43,44]. Entering into details, the head of the emissometer is allowed to slide above the sample in order to prevent the measured surface from warming up during the test session. The sliding operation is carried out by hand and time is needed to achieve a stabilized output of the instrument, therefore the measurement may be time-consuming; moreover, it may be affected by the operator’s expertise. An approach was recently proposed [45] to solve both problems, based on automating the sliding operation by means of a robotized arm, and acquiring the voltage output returned by the emissometer by means of a computerized data acquisition system that allows visualization of its time-evolution pattern and may also interact with the robot. The approach has eventually provided encouraging results, with measurements in very good agreement with manual operation and also excellent repeatability. It is worth mentioning that the slide method is not specified in ASTM C1371 [39], but only in the technical notes of the instrument’s producer [43,44].

The emissometer based on EN 15976 Standard [40], also known as ‘TIR emissometer’, is again based on a hot head that embeds a hemispherical cavity kept at a temperature significantly higher than that of the sample, which must instead be as close as possible to the ambient temperature. The head is placed onto the sample and the infrared radiation emitted by the cavity and reflected by the sample surface is measured by a fast response sensor viewing the surface from the bottom of the cavity, with near-normal orientation. The acquired signal is clearly correlated to the infrared reflectance of the sample surface, which is, for opaque surfaces, the complement to 1 of the emittance at the same temperature. It is acquired immediately after the head is placed onto the sample, so there is no time for the sample surface to significantly warm up and a low thermal conductivity of the support material does not disturb the measurement. A calibration is again performed before each test, automatically managed by the instrument, by measuring two reference samples with known emittances, a polished metal plate and a black anodized finned surface. The producer of the TIR emissometer (which provided two reference samples with emittance  $\varepsilon_{\text{low}} = 0.011$  and  $\varepsilon_{\text{high}} = 0.964$ ) ensures uncertainty  $\pm 0.01$  or better in the range  $0.02 < \varepsilon_s < 0.98$ .

While the term ‘emissivity’ is generically mentioned in the EN 15976 Standard, without further specification, the TIR emissometer measures the near-normal thermal emittance. For the most common case of non-metallic surfaces, the near-normal thermal emittance is slightly higher than the hemispherical emittance, the one relevant for surface overheating and to be used for SRI calculation. Data from [46] are plotted in Figure 13, showing that the overestimation may be as high as 0.045–0.055 for dielectric samples with high emittance, so the use of near-normal emittance values for cool roofing or cool pavement products may result in an unfair overestimation with respect to hemispherical emittance values measured by the alternative method.

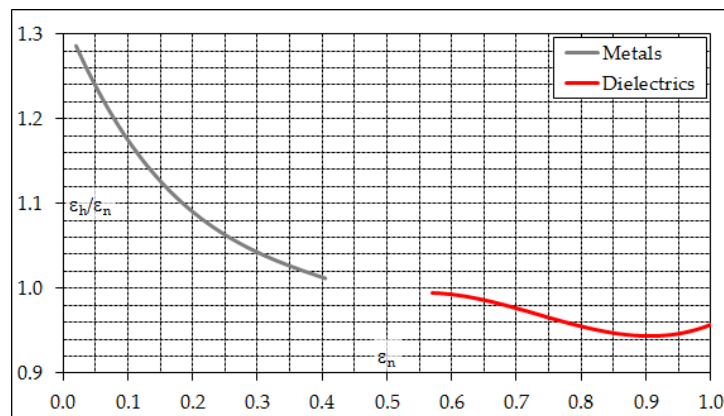


**Figure 13.** Hemispherical vs. near-normal emittance.

Near-normal emittance  $\varepsilon_n$  measured according to EN 15976 can be converted in hemispherical emittance  $\varepsilon_h$  by interpolating the data plotted in Figure 13 through the following formulas [46,47], respectively for dielectrics

$$\frac{\varepsilon_h}{\varepsilon_n} = 0.1569 + 3.7669 \cdot \varepsilon_n - 5.4398 \cdot \varepsilon_n^2 + 2.4733 \cdot \varepsilon_n^3 \quad (20)$$

and for metals

$$\frac{\varepsilon_h}{\varepsilon_n} = 1.3217 - 1.8766 \cdot \varepsilon_n + 4.6586 \cdot \varepsilon_n^2 - 5.8349 \cdot \varepsilon_n^3 + 2.7406 \cdot \varepsilon_n^4 \quad (21)$$

An advantage of the TIR emissometer on the thermal emissometer is that it does not require a time-consuming procedure such as the slide method with samples having a low thermal conductivity, as with all pavement products and most of roofing products apart from coated metals. On the other hand, the minimum size of the sample, imposed by the size of the hot head, is about 100 mm for the TIR emissometer versus some 60 mm for the thermal emissometer, even less when using optional port adapters [48]. Nevertheless, application of the slide method requires a size of the sample surface multiple of that of the emissometer head in order to allow space enough for the head itself to slide above the surface without progressively warming it up. The abovementioned port adapter helps in lowering the sample size, in principle making it possible to test the 10 cm × 10 cm samples required for accelerated ageing by ASTM D7897 [32].

Thermal emittance of high-emittance products is marginally affected by soiling,  $\pm 0.05$  at most according to data in the CRRC database [49], but the plots in Figures 2 and 12 show that the effect on the SRI value is generally lower than  $\pm 1$ . Moreover, thermal emittance generally increases, up to 0.07, in low-emittance products [49]. Therefore, it may be reasonable, even if not necessarily precautionary, to assume the thermal emittance is constant after ageing, unless values measured on samples subjected to natural or accelerated ageing are available.

### 3.4. Combined Effects of Measurement Issues

As explained in Section 3.2, using the E891BN spectrum may yield an apparent increase of solar reflectance with respect to AM1GH or EN410G as high as 0.02 for highly reflective surfaces with  $\rho_{\text{sol}} \approx 0.8$  (see Table 2). The increase may be 0.01 with respect to G173GT, but negligible with respect to G173DN. For more absorbing surfaces with  $\rho_{\text{sol}} \approx 0.4$  use of the E891BN spectrum may yield an even higher apparent increase with respect to AM1GH or AN410G, up to 0.03–0.04, especially if those surfaces show selective behavior, i.e., the reflectivity spectrum is sharply different between visible and near infrared ranges. In Section 3.3 it is also explained that for high emittance surfaces with  $\varepsilon_e \approx 0.9$  using the direct normal thermal emittance instead of the hemispherical one yields an apparent increase

in the emittance as high as 0.055. Combining the two increases may yield significant discrepancies in the calculated SRI values, exemplified in Figure 14 for two categories of material: (a) highly reflective materials such as those used for flat roofs; and (b) moderately reflective materials such as those used for pitched roofs and pavements. With highly reflective surfaces, the SRI values calculated with AM1GH/EN410G spectra and hemispherical emittance may easily be lower by 3.5 points than those calculated with E891BN/G171DN spectra and near-normal emittance. The discrepancy may even rise to 7.5 points for moderately reflective surfaces. All this clearly applies to both new and aged samples.

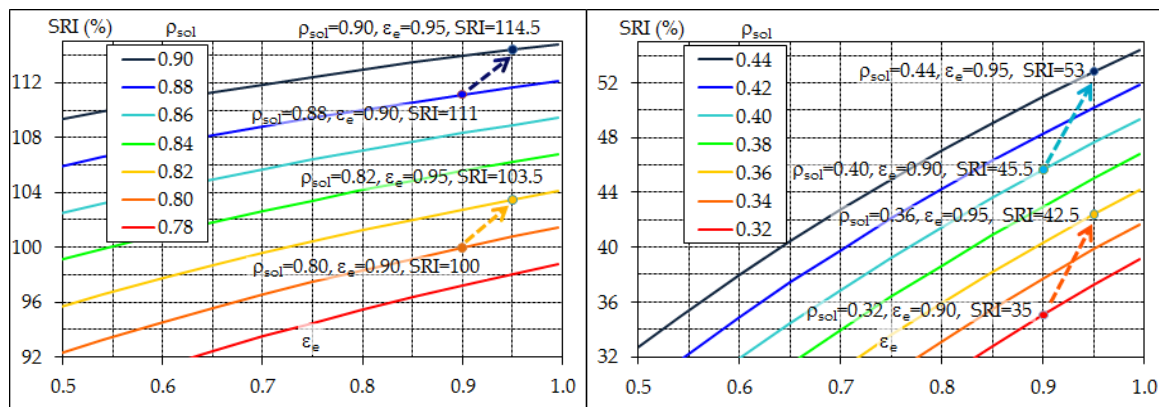


**Figure 14.** Theoretical discrepancies of calculated SRI values for intermediate wind speed ( $2 \text{ m/s} < v_{wind} < 6 \text{ m/s}$ ,  $h_{ce} = 12 \text{ W}/(\text{m}^2 \text{ K})$ ) and (from left to right) highly reflective and moderately reflective surfaces.

All analyses of Sections 3.2–3.4 do not concern the uncertainty of measurement, which in the authors' experience can be low provided that the test methods are thoroughly implemented and calibration standards are properly chosen and maintained. This requisite should be automatically fulfilled when a laboratory operates under ISO/IEC 17025 accreditation.

#### 4. Conclusive Remarks

- The SRI has raised significant interest in the construction sector thanks to its relative ease of calculation and, above all, its effective representation of the thermal behavior of a built surface subjected to solar radiation.
- A linear correlation exists between SRI and both the surface temperature and the fraction of incident solar heat that is transferred to the near ground air. Since a given SRI value can be the result of different pairs of solar reflectance and thermal emittance values, SRI seems a more effective indicator than solar reflectance alone for comparative evaluation of the capability of built surfaces to limit urban warming.
- SRI calculation is based on the hypothesis of an adiabatic irradiated surface and does not consider the insulation or the inertia of the materials below; nonetheless it can work well as an indicator of the heat transmitted to the external near ground air, and therefore of the contribution to urban warming, since the heat flow rate conducted through a roof or into the ground can be lower by one or two orders of magnitude than solar irradiance.
- Values of the convection heat transfer coefficient specified for SRI calculation are arbitrary; nonetheless they are in good agreement with the literature and are therefore reasonable from the perspective of product comparison.
- The standard solar spectra currently recommended in the U.S. by CRRC and allowed in Europe by ECRC to calculate the weighted average of surface reflectivity, considering air mass 1.5 and direct normal radiation, are probably improper for the prediction of annual peak solar heat gain; thus, spectra for air mass 1 global radiation on a horizontal surface have been recommended in

recent studies. On the other hand, the adoption of such spectra was shown to lower the measured performance by a non-negligible amount and to potentially inhibit a fair comparison between newly rated and already rated products. The issue still needs to be properly addressed.

- Two test methods of practical relevance are available to measure thermal emittance, one (ASTM C1371) returning a hemispherical value and the other (EN 15976) a near-normal value. Unless properly corrected, near-normal emittance may represent a non-negligible overestimation of hemispherical emittance, the one relevant to infrared heat transfer between a built surface and the sky.
- The combined use of air mass 1.5 direct normal radiation spectra and near-normal emittance can lead to a significant overestimation of SRI with respect to using air mass 1 global horizontal radiation spectra and hemispherical emittance, especially for surfaces with high or intermediate solar reflectance. The freedom of choice apparently allowed by standard test methods and rating systems may induce such an unfair situation.
- The surface performance achieved after ageing is relevant to the long-term behavior of built surfaces and therefore this should be considered in regulations rather than that initially measured. Nonetheless at least three years are needed for natural ageing—a requisite that is not easily accepted by the industry—and randomly variable conditions are also possible in the weathering sites due to variations in meteorology and air pollution.
- In many countries different from the U.S. the regulations on solar reflective materials are still under development and only initial values of surface properties are considered, or can be provided by product manufacturers. On the other hand, a fast improvement of commercial products and regulations may be impeded by the long time required for natural ageing.
- A recently developed laboratory test method for accelerated ageing—already a standard test method—makes it possible to condense into three days the three-year long process of natural ageing required by CRRC. It proved to be easy and fast to perform, repeatable, and, above all, able to reproduce the reflectance obtained in a wide range of naturally exposed roofing products.
- In order to create a fair global market for solar reflective products, as well as to favor their use where this is still undeveloped, a general alignment is required on measurement methods. The use of a common solar spectrum is desirable for solar reflectance measurement, possibly representative of peak heat load conditions. The use of hemispherical thermal emittance should also be clearly specified. Under these conditions, the effects of both reflectance and emittance can be effectively summarized by the SRI. In order to consider aged values of SRI—that is, those relevant to the long term performance of built surfaces—worldwide use of an accelerated soiling method such as that specified by ASTM D7897 may greatly speed up the development and qualification of durable products, thus favoring the diffusion of specific performance limits intended to improve building energy efficiency and limit urban warming.

**Acknowledgments:** The research was partially funded by Fondazione Cassa di Risparmio di Modena, which supported the development of the Energy Efficiency Laboratory (EELab) of the University of Modena and Reggio Emilia. The author also wishes to acknowledge personnel of EELab and members of the Technical Committee of the European Cool Roof Council for the useful discussions that provided hints and support to the development of the present work.

**Conflicts of Interest:** The author declares no conflict of interest. The founding sponsor had no role in the design of the study; in the collection, analyses, or interpretation of data; in the writing of the manuscript, and in the decision to publish the results.

## References

1. United Nations. *World Urbanization Prospects: 2014 Revision*; United Nations: New York, NY, USA, 2014.
2. Santamouris, M. Analyzing the heat island magnitude and characteristics in one hundred Asian and Australian cities and regions. *Sci. Total Environ.* **2015**, *512–513*, 582–598. [[CrossRef](#)] [[PubMed](#)]

3. NASA—Goddard Institute for Space Studies. *NASA-GISS, 2017. GISS Surface Temperature Analysis (GISTEMP)*; NASA—Goddard Institute for Space Studies: New York, NY, USA, 2017.
4. Santamouris, M. Regulating the damaged thermostat of the cities—Status, impacts and mitigation challenges. *Energy Build.* **2015**, *91*, 43–56. [[CrossRef](#)]
5. Santamouris, M.; Cartalis, C.; Synnefa, A.; Kolokotsa, D. On the impact of urban heat island and global warming on the power demand and electricity consumption of buildings—A review. *Energy Build.* **2015**, *98*, 119–124. [[CrossRef](#)]
6. Akbari, H.; Pomerantz, M.; Taha, H. Cool surfaces and shade trees to reduce energy use and improve air quality in urban areas. *Sol. Energy* **2001**, *70*, 295–310. [[CrossRef](#)]
7. Akbari, H.; Cartalis, C.; Kolokotsa, D.; Muscio, A.; Pisello, A.L.; Rossi, F.; Santamouris, M.; Synnefa, A.; Wong, N.H.; Zinzi, M. Local climate change and urban heat island mitigation techniques—The state of the art. *J. Civ. Eng. Manag.* **2016**, *22*, 1–16. [[CrossRef](#)]
8. European Committee for Standardization (CEN). *EN ISO 13786:2007—Thermal Performance of Building Components—Dynamic Thermal Characteristics—Calculation Methods*; European Committee for Standardization (CEN): Brussels, Belgium, 2007.
9. ASTM International. *ASTM E1980-11—Standard Practice for Calculating Solar Reflectance Index of Horizontal and Low Sloped Opaque Surfaces*; ASTM International: West Conshohocken, PA, USA, 2011.
10. U.S. Green Building Council. *LEED v4 for Building Design and Construction*; (updated July 8, 2017); U.S. Green Building Council: Washington, DC, USA.
11. California Energy Commission. *2016 Building Energy Efficiency Standards for Residential and Nonresidential Buildings—Title 24, Part 6, and Associated Administrative Regulations in Part 1*; California Energy Commission: Sacramento, CA, USA, 2015.
12. Environmental Protection Agency. *ENERGY STAR® Program Requirements—Product Specification for Roof Products—Eligibility Criteria—Version 3.0*; Environmental Protection Agency: Washington, DC, USA, 2013.
13. Muscio, A.; Akbari, H. An index for the overall performance of opaque building elements subjected to solar radiation. *Energy Build.* **2017**, *157*, 184–194. [[CrossRef](#)]
14. Cool Roof Rating Council. *ANSI/CRRC S100 (2016)—Standard Test Methods for Determining Radiative Properties of Materials, Properties of Materials*; Cool Roof Rating Council: Portland, OR, USA, 2016.
15. European Cool Roof Council. *Product Rating Manual*; (November 2014); European Cool Roof Council: Brussels, Belgium, 2014.
16. European Committee for standardization (CEN). *EN ISO/IEC 17025:2005—General Requirements for the Competence of Testing and Calibration Laboratories*; European Committee for standardization (CEN): Brussels, Belgium, 2005.
17. European Committee for standardization (CEN). *EN ISO 6946:2007—Building Components and Building Elements—Thermal Resistance and Thermal Transmittance—Calculation Method*; European Committee for standardization (CEN): Brussels, Belgium, 2007.
18. American Society of Heating, Refrigerating and Air-Conditioning Engineers. *ASHRAE Handbook Fundamentals 2009*; (SI edition); American Society of Heating, Refrigerating and Air-Conditioning Engineers: Atlanta, GA, USA, 2009.
19. Kakaç, S.; Shah, R.K.; Aung, W. (Eds.) *Handbook of Single-Phase Convective Heat Transfer*; Wiley-Interscience: New York, NY, USA, 1987; ISBN 978-0-47-181702-4.
20. Incropera, F.P.; De Witt, D.P. *Fundamentals of Heat and Mass Transfer*, 5th ed.; John Wiley and Sons: Hoboken, NJ, USA, 2005; ISBN 978-0-47-138650-6.
21. ASTM International. *ASTM E903-12—Standard Test Method for Solar Absorptance, Reflectance, and Transmittance of Materials Using Integrating Spheres*; ASTM International: West Conshohocken, PA, USA, 2012.
22. European Committee for Standardization (CEN). *EN 410:2011—Glass in Building—Determination of Luminous and Solar Characteristics of Glazing*; European Committee for Standardization (CEN): Brussels, Belgium, 2011.
23. Levinson, R.; Akbari, H.; Berdahl, P. Measuring solar reflectance—Part I: Defining a metric that accurately predicts solar heat gain. *Sol. Energy* **2010**, *84*, 1717–1744. [[CrossRef](#)]
24. Levinson, R.; Akbari, H.; Berdahl, P. Measuring solar reflectance—Part II: Review of practical methods. *Sol. Energy* **2010**, *84*, 1745–1759. [[CrossRef](#)]

25. ASTM International. *ASTM C1549-09 (Reapproved 2014)—Standard Test Method for Determination of Solar Reflectance Near Ambient Temperature Using a Portable Solar Reflectometer*; ASTM International: West Conshohocken, PA, USA, 2014.
26. ASTM International. *ASTM E891-87(1992)—Tables for Terrestrial Direct Normal Solar Spectral Irradiance Tables for Air Mass 1.5 (Withdrawn 1999)*; ASTM International: West Conshohocken, PA, USA, 1992.
27. ASTM International. *ASTM G173-03(2012)—Standard Tables for Reference Solar Spectral Irradiances: Direct Normal and Hemispherical on 37° Tilted Surface*; ASTM International: West Conshohocken, PA, USA, 2012.
28. Berdahl, P.; Akbari, H.; Levinson, R.; Miller, W.A. Weathering of roofing materials—An overview. *Constr. Build. Mater.* **2008**, *22*, 423–433. [[CrossRef](#)]
29. Sleiman, M.; Ban-Weiss, G.; Gilbert, H.E.; Francois, D.; Berdahl, P.; Kirchstetter, T.W.; Destailats, H.; Levinson, R. Soiling of building envelope surfaces and its effect on solar reflectance—Part I: Analysis of roofing product databases. *Sol. Energy Mater. Sol. Cells* **2011**, *95*, 3385–3399. [[CrossRef](#)]
30. Sleiman, M.; Kirchstetter, T.W.; Berdahl, P.; Gilbert, H.E.; Quelen, S.; Marlot, L.; Preble, C.V.; Chen, S.; Montalbano, A.; Rosseler, O.; et al. Soiling of building envelope surfaces and its effect on solar reflectance—Part II: Development of an accelerated aging method for roofing materials. *Sol. Energy Mater. Sol. Cells* **2014**, *122*, 271–281. [[CrossRef](#)]
31. Sleiman, M.; Chen, S.; Gilbert, H.E.; Kirchstetter, T.W.; Berdahl, P.; Bibian, E.; Bruckman, L.S.; Cremona, D.; French, L.H.; Gordon, D.A.; et al. Soiling of building envelope surfaces and its effect on solar reflectance—Part III: Interlaboratory study of an accelerated aging method for roofing materials. *Sol. Energy Mater. Sol. Cells* **2015**, *143*, 581–590. [[CrossRef](#)]
32. ASTM International. *ASTM D7897-15—Standard Practice for Laboratory Soiling and Weathering of Roofing Materials to Simulate Effects of Natural Exposure on Solar Reflectance and Thermal Emittance*; ASTM International: West Conshohocken, PA, USA, 2015.
33. ASTM International. *ASTM E1918-16—Standard Test Method for Measuring Solar Reflectance of Horizontal and Low-Sloped Surfaces in the Field*; ASTM International: West Conshohocken, PA, USA, 2016.
34. Levinson, R.; Berdahl, P.; Akbari, H.; Miller, W.A.; Joedicke, I.; Reilly, J.; Suzuki, Y.; Vondran, M. Methods of creating solar-reflective nonwhite surfaces and their application to residential roofing materials. *Sol. Energy Mater. Sol. Cells* **2007**, *91*, 304–314. [[CrossRef](#)]
35. Rosenfeld, A.H.; Akbari, H.; Bretz, S.; Fishman, B.L.; Kurn, D.M.; Sailor, D.; Taha, H. Mitigation of urban heat islands: Materials, utility programs, updates. *Energy Build.* **1995**, *22*, 255–265. [[CrossRef](#)]
36. Bretz, S.; Akbari, H.; Rosenfeld, A.H. Practical issues for using solar-reflective materials to mitigate urban heat islands. *Atmos. Environ.* **1998**, *32*, 95–101. [[CrossRef](#)]
37. Libbra, A.; Muscio, A.; Siligardi, C.; Tartarini, P. Assessment and improvement of the performance of antisolar surfaces and coatings. *Prog. Org. Coat.* **2011**, *72*, 73–80. [[CrossRef](#)]
38. Libbra, A.; Muscio, A.; Siligardi, C. Energy performance of opaque building elements in summer: Analysis of a simplified calculation method in force in Italy. *Energy Build.* **2013**, *64*, 384–394. [[CrossRef](#)]
39. ASTM International. *ASTM C1371-15—Standard Test Method for Determination of Emittance of Materials Near Room Temperature Using Portable Emisometers*; ASTM International: West Conshohocken, PA, USA, 2015.
40. European Committee for standardization (CEN). *EN 15976—Flexible sheets for waterproofing—Determination of emissivity*; European Committee for standardization (CEN): Brussels, Belgium, 2011.
41. Kollie, T.G.; Weaver, F.J.; McElroy, D.L. Evaluation of a commercial, portable, ambient temperature emissometer. *Rev. Sci. Instrum.* **1990**, *61*, 1509–1517. [[CrossRef](#)]
42. Devices & Services Co. *D&S Technical Note 92-11—Emisometer Model. AE—Hemispherical vs Normal Emittance*; Devices & Services Co.: Dallas, TX, USA, 1992.
43. Devices & Services Co. *D&S Technical Note 04-1—Emisometer Model AE—Slide Method for AE Measurements*; Devices & Services Co.: Dallas, TX, USA, 2004.
44. Devices & Services Co. *D&S Technical Note 10-2—Emisometer Model AE1—Slide Method for High. Emittance Materials with Low Thermal Conductivity*; Devices & Services Co.: Dallas, TX, USA, 2010.
45. Pini, F.; Ferrari, C.; Libbra, A.; Leali, F.; Muscio, A. Robotic implementation of the slide method for measurement of thermal emissivity of building elements. *Energy Build.* **2016**, *114*, 241–246. [[CrossRef](#)]
46. Rubin, M.; Arasteh, D.; Hartmann, J. A correlation between normal and hemispherical emissivity coatings on glass. *Int. Commun. Heat Mass Transf.* **1997**, *14*, 561–565. [[CrossRef](#)]

47. National Fenestration Rating Council Inc. *NFRC 301-2014[E0A0]—Standard Test Method for Emittance of Specular Surfaces Using Spectrometric Measurements*; National Fenestration Rating Council Inc.: Greenbelt, MD, USA.
48. Devices & Services Co. *D&S Technical Note 11-2—Model. AE1 Emittance Measurements Using a Port. Adapter, Model. AE-ADP*; Devices & Services Co.: Dallas, TX, USA, 2011.
49. Paolini, R.; Zinzi, M.; Poli, T.; Carnielo, E.; Mainini, A.G. Effect of ageing on solar spectral reflectance of roofing membranes: Natural exposure in Roma and Milano and the impact on the energy needs of commercial buildings. *Energy Build.* **2014**, *84*, 333–343. [[CrossRef](#)]



© 2018 by the author. Licensee MDPI, Basel, Switzerland. This article is an open access article distributed under the terms and conditions of the Creative Commons Attribution (CC BY) license (<http://creativecommons.org/licenses/by/4.0/>).